Mohamed ARROUF, Farida BENABID

University of Batna, Algeria

Photovoltaic Pumping System Based on Intel 80C196KC Microcontroller

Abstract. *Solar energy is of increasing interest in pumping system applications particularly in isolated area.* Enhancement of pumping system efficiency depends on optimization of solar energy generation and system consumption. *This paper presents an optimally designed and realized solar pumping system which can be used for irrigation, under variation of climate conditions in remote areas, far away from electric grid. The solar pumping system is built at the laboratory level and the tests show correct operation of the proposed system.*

Streszczenie. *Energia słoneczna cieszy się większym zainteresowaniem jako źródło energii dla systemów pompowania wody, szczególnie w odizolowanych regionach. Zwiększenie wydajności pompowania systemu zależy od optymalizacji pozyskiwania energii słonecznej i zużycie energii przez system. W artykule przedstawiono optymalnie zaprojektowany i zrealizowany słoneczny system pompowania, który może być zastosowany do nawadniania, z uwzględnieniem zmienności warunków klimatycznych w odległych obszarach, z dala od sieci elektrycznej. Układ słoneczny pompowania jest zbudowany w laboratorium a testy wykazują prawidłowe działanie proponowanego systemu. (**System pompowania zasilanego energią fotowoltaiczną zrealizowany za pomocą mikrokontrolera Intel 80C196KC**).*

Keywords: Photovoltaic generators, MPPT, inverter, motor –driven pump.
Słowa kluczowe: generator fotowoltaiczne, MPPT, przekształtnik, pompa napędzana silnikiem elektrycznym

Introduction

The utilization of photovoltaic conversion to power water pumps is today an emerging technology, characterized by gradually declining costs. In remote areas far away from the electric grid, the use of photovoltaic pumping systems for irrigation is today economically advantageous. Algeria is a large country with the area of about 2.4 millions square km with diverse climatic conditions. Solar energy represents a significant potential in Algeria. In fact, the country receives more than 3000h of sunshine per year with a high level of irradiation [1].

Obviously, photovoltaic generators are classified as nonlinear electrical sources since the output power is affected by the weather conditions such as irradiance level and temperature which changes randomly in time. The optimization of the photovoltaic pumping system is based upon the optimization of the power delivered by the photovoltaic generator; this is done by the maximum power point tracking (MPPT) and the optimization of the induction motor operation which is completed by the application of a nearly constant voltage-to-frequency-ratio control technique.

System layout

The schematic diagram of the realized photovoltaic pumping system is proposed in fig.1. As shown in the figure, the system consists of a photovoltaic generator which presents the power supply source. A boost chopper, which is used as an MPPT, connected to a pulse width modulation (PWM) controlled voltage source inverter, which converts the DC voltage to AC voltage in order to feed the three-phase induction motor. The MPPT control strategy and the inverter PWM switching pattern are implemented in the microcontroller as a program.

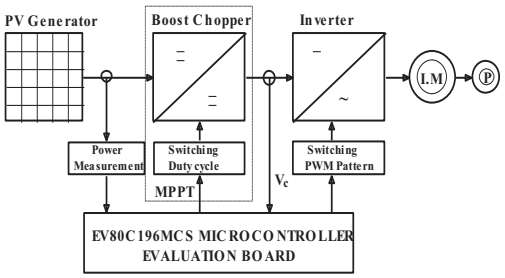

Fig.1. Block diagram of PV pumping system

Photovoltaic generator

A photovoltaic generator consists of a number of modules, formed by the interconnection of photovoltaic cells, connected together in series and parallel to provide the required voltage and current. The generator sizing therefore depends on the connexion variability of the modules that constitute the generator and the cells that comprise the modules. Photovoltaic cells convert the solar radiation into electrical energy. The conversion is however limited to the spectrum of solar radiation that can be utilized.

a)

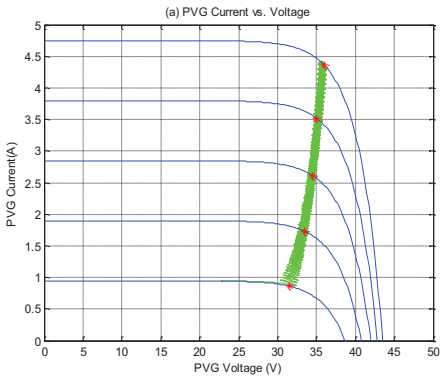

b)

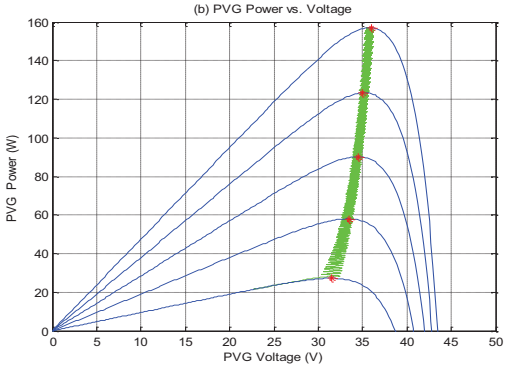

Figure.2. Current-voltage characteristics of PVG with MPPT for five irradiance levels (a) and Power–voltage (b)

For the photovoltaic generator composed of N_p modules in parallel and N_s in series, the I-V equation is given by (1) [2].

(1) $$I_g = N_p I_{ph} - N_p I_{Sat}\left\{\exp\left[\frac{q}{AKTN_S}\left(V_g + I_g R_S\right)\right] - 1\right\}$$

where: I_g, V_g - output current and voltage respectively, I_{ph} - generated current under given radiation, I_{sat}- saturation current, q-charge of electron, k- Boltzmann's constant, R_s - series resistance, A -ideality factor of the P-N junction.

Fig.2 shows photovoltaic generator characteristics current- voltage I-V and power voltage P-V with MPPT a as a function of solar irradiance.

Maximum power point tracking

The maximum power tracking is the essential element in the optimization of photovoltaic pumping systems since the photovoltaic generator is a non-linear energy source. In order to optimize the electrical operating conditions of the generator, it is necessary to use a specialized device. This device, maximum power point tracker, consists of a power section and a control section. The power section is generally a DC/DC converter whereas the control section can be built either of digital or analog electronics.

A. DC/DC Converter

The boost converter is used to exactly track the maximum power point rather than maximizing the voltage. The basic circuit of the boost converter designed and developed is shown in fig.3.

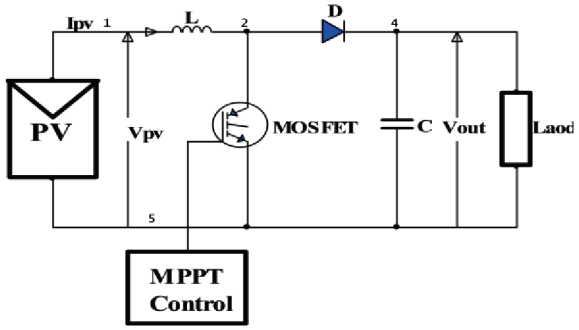

Fig.3. Step- up chopper

It is well known that the relationship between the input voltage and the output voltage of the boost converter is given by formula (2).

(2) $$V_{out} = V_{PV}/(1-\alpha)$$

where $\alpha = t_{on}/T$ is defined as the converter duty cycle. This means that the converter output voltage can be simply controlled by the variation of the duty cycle. In order to track the maximum power point of the photovoltaic generator the duty cycle α is either increased or decreased.

The inductor value, L, required to operate the converter continuously in conduction mode is calculated such that the peak inductor current at maximum output power does not exceed the power switch current rating. Hence, L is calculated from the relationship (3).

(3) $$L \geq V_{pv}\alpha / f\Delta I_{pv}$$

where: $f=1/T$ - switching frequency,α - duty cycle at maximum converter output power, V_{pv} - input voltage and ΔI_{pv} -peak-to-peak inductor ripple current.

The choice of the converter inductor value and the switching frequency is a compromise between converter efficiency, cost, power capability and weight.

The output capacitor required value that maintain the desired peak-to- peak output voltage ripple is calculated from the relationship (4).

(4) $$C \geq I_{out}\alpha / f\Delta V_{out}$$

where: $f=1/T$ - switching frequency, I_{out} - output current , ΔV_{out} - peak-to-peak ripple capacitor output voltage.

Converter control circuit

The system control circuit shown in fig.4 is based on the Intel 80C196KC Microcontroller and the control circuit consists of:

- Interface circuits which contain sensors and signal conditioners connected to the microcontroller A/D converter;
- Intel 80C196KC microcontroller
- Quadruple differential line driver
- IC driver for power MOSFET.

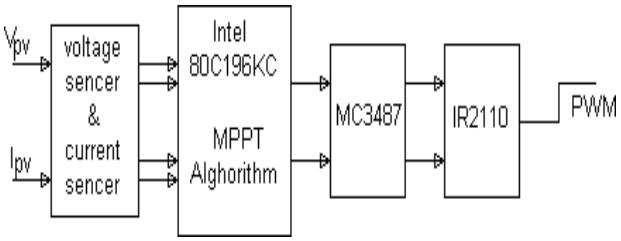

Fig.4 Converter control circuit

B-Tracking Technique

Several techniques have been proposed in order to drive an AC or DC loads at the maximum power point [3]. These techniques are based on the regulation of the photovoltaic generator output voltage or current according to a reference voltage or current signal, which is either constant or derived from the PV generator characteristics. A characteristic point of these techniques is to directly use the DC\DC converter duty cycle as a control parameter and force the derivative $dP/d\alpha$ to zero, where P is the PV array output power and α the duty cycle [4, 5]. This kind of MPPT technology simplifies the system control structure to one control loop as shown in fig.5.

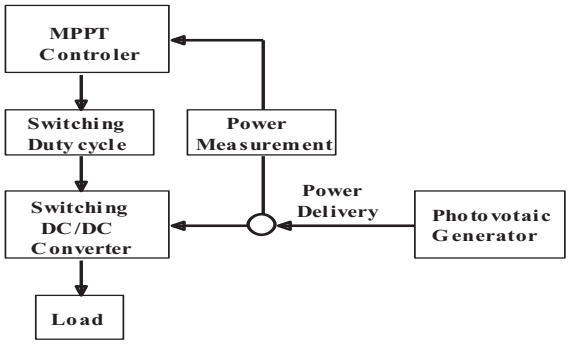

Fig.5. Block diagram of the MPPT control

The control technique flowchart is shown in fig.6. Slope is a program variable with values either 1 or -1 indicating the direction that must follow on the P-α curve in order to increase the output power. While d represents the increment step of duty cycle, which is a constant number between 0 and 1, and P and α represent the power level

and duty cycle value respectively. Given that an 8-bit CPU register is used to store the PWM duty cycle in the present application, the d value is made equal to 1/256.

In or application, an EV80C196MCS Microcontroller Evaluation Board is used as a tool of control the duty cycle of the DC/DC converter and therefore the PV output power. This is done through the reading of the instantaneous PV generator output voltage and current, so the power can be calculated and compared to the previous PV generator output power. Depending on the result of the comparison the duty cycle is changed accordingly and the process is repeated until the maximum power point has been reached as shown in fig 7.

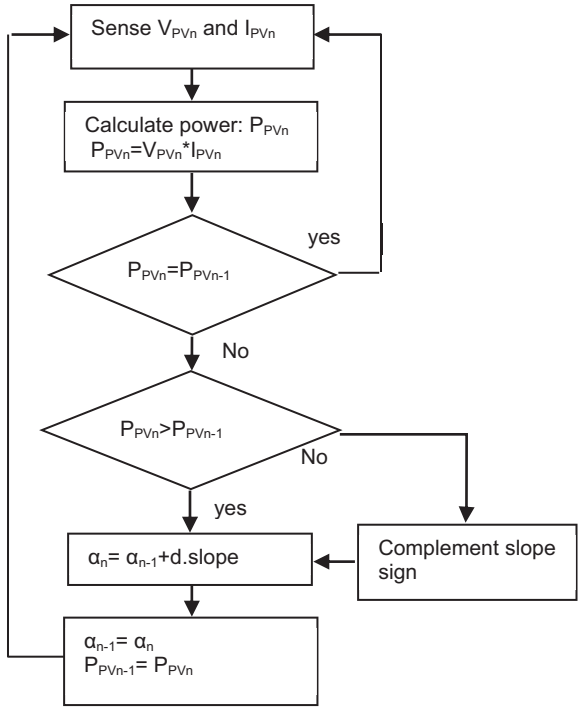

Fig.6. MPPT control technique flowchart

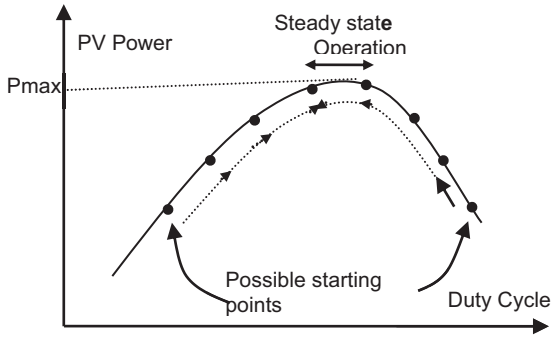

Fig.7. MPPT tracking process

Voltage source inverter

The voltage source inverter is used to supply the induction motor driving a centrifugal pump [7]. The utilized Mitsubishi Intelligent Power Module PM10CSJ060 inverter shown in fig.8 is an isolated base module designed for power switching applications at frequencies up to 20 kHz with a built-in control circuits which provide optimum gate driving and protection logic for IGBTs against:

– Short Circuit
– Over Current
– Over Temperature
– Under Voltage

The intelligent power module is specially designed for variable speed motor control and is characterized by high frequency and highly efficient operation. The inverter output voltage is controlled by a sinusoidal pulse - width modulation (PWM) control technique in which a high frequency symmetrical triangular carrier wave is compared to a synchronized sine wave modulating reference wave with the required output frequency.

The sinusoidal (PWM) control technique is generated by the microcontroller in such a way that the inverter output voltage-to-frequency ratio is maintained constant. Due to the fluctuation of the maximum input power produced by the photovoltaic generator through the MPPT according to the solar radiation level and temperature, the inverter output power is variable.

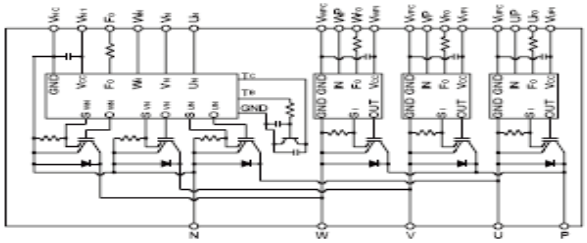

Fig. 8. PM10CSJ060 inverter internal circuit

Induction motor operation

To produce a starting torque, and subsequently a running torque, it is necessary to have a current flowing through the rotor winding by short circuiting the winding. Initially the induced e.m.f. from the inverter causes a rotor current per phase I_R to flow through the short circuit, and acts with the flux field to produce the starting torque. The sense of this torque is always to cause the rotor to run in the same direction as the rotating field. The flux field is assumed to revolve at a speed corresponding to the applied stator frequency and the poles of the stator winding. This speed is called the synchronous speed and is given by (5):

$$\omega_S = 2\,\omega/P \tag{5}$$

where: ω - stator or source frequency in rad/s , P - number of poles.

The relative speed between the rotor and the flux wave or the slip is defined by (6).

$$S = (\omega_S - \omega_R)/\,\omega_S \tag{6}$$

where: ω_R - motor operating speed.

Using the equivalent circuit of the induction motor shown in fig. 9 the torque equation is given by (7) [8].

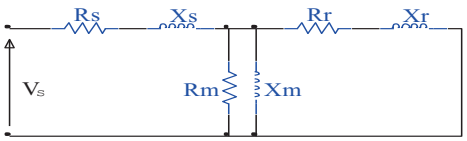

Fig 9. Induction motor equivalent circuit

$$T = 3Pk\frac{\omega_R X_m^2 / R_R}{\left[R_s - \frac{\omega_R}{SR_R}\left(X_{11}X_{22} - X_m^2\right)\right]^2 + \left[X_{11} + \frac{\omega_R R_S X_{22}}{\omega_S R_R}\right]^2} \tag{7}$$

where : K - terminal voltage frequency ratio, p - number of pole pairs, ω_R -rotor frequency = $S\omega_S$, X_{11} =$X_m + X_S$, X_{22} =X_m+X_R, X_m- mutual reactance at rated supply frequency,

X_R, X_S - stator and rotor leakage reactances , respectively, S- motor slip.

The speed of the induction motor can be controlled by changing the supply frequency. Nevertheless the terminal voltage can be considered proportional to the product of frequency and the flux. If the voltage is maintained fixed at its rated value while the frequency is reduced below its rated value, the flux will increase. This would cause saturation of the air-gap flux. At low frequency the reactance will decrease and the motor current may be too high. In order to avoid saturation and to minimize losses, motor is operated at rated air-gap flux by varying terminal voltage with frequency so as to maintain the ratio (V_s /ω_s) nearly constant [9,10,11].

For the motor optimum efficiency operation, the ratio of the supply voltage applied to the induction motor and its frequency (V_s /ω_s) is adjusted in order to operate the motor at highest efficiency.

From the equivalent circuit, the total mechanical power of a motor is given by (8):

$$P_m = 3I_R^2 R_R (1-S)/S \tag{8}$$

Hence, the efficiency

$$\eta = \left[I_R^2 R_R (1-S)/S\right] / I_S^2 R_{in} \tag{9}$$

By differentiating the efficiency expression with respect to the slip S, and equating to zero, an optimum slip which yields the maximum efficiency is obtained and given by (10):

$$S_{op} = \left(R_R / X_m + X_R\right)\sqrt{(1+A)} / \left(1 + R_R / R_S\right) \tag{10}$$

where: $A = X_m^{\,2} / R_S R_m$, R_m -core loss resistance.

Motor operation at S_{op} implies that the input impedance, the power factor, and the motor efficiency are constant. The optimum mechanical speed is given by (11):

$$\omega_{mop} = (1 - S_{op})\omega_s / p. \tag{11}$$

Centrifugal pump

The pump represents the mechanical load of the induction motor and its size identifies the power rating of the other system component. The utilized pump is single stage centrifugal which can be characterized by (12) and (13) [8].

$$P_P = \rho\, g\, HQ \tag{12}$$

$$\eta_P = P_P / P_{mech} \tag{13}$$

where: P_P -pump hydraulic output power in W, ρ-water density in kg/m^2, g - gravitation acceleration in m/s^2 , Q-flow rate in m^3/h, H - pumping height in meters m, η_P - pump efficiency, P_{mech} pump input mechanical power.

Experimental results

To illustrate the performance of the designed and implemented system at the laboratory level, tests have been carried out on the system in order to verify the I operation of the DC/DC converter, the MPPT tracking system algorithm and induction motor supply voltage and line current.

The efficiency of the DC/DC converter is found to be about 94%. Fig. 10 shows the simulated and practical test results of the realized inverter. It can be observed that the simulated and the real data curves of the efficiency are comparable.

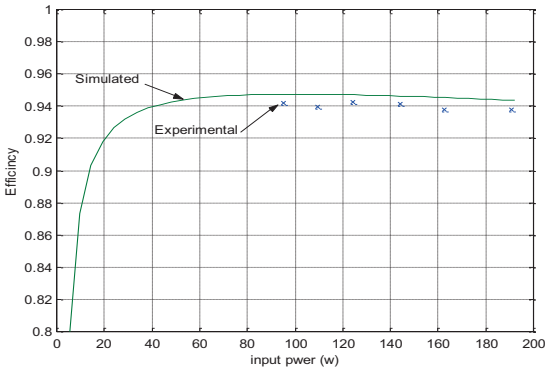

Fig.10. DC/DC converter, simulated and experimental efficiency curves.

Figure.11 illustrates the converter output power and input power against the duty cycle. It can be seen from the figure that the converter losses at the duty cycle 0.5 are higher than any other duty cycle values.

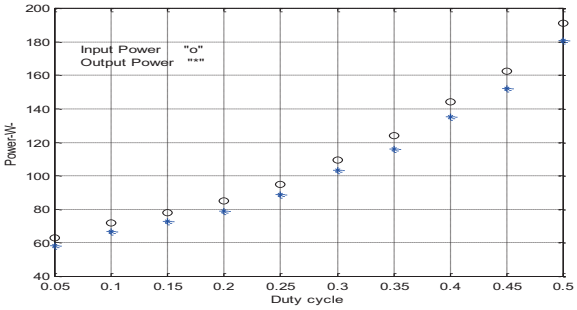

Fig 11.Converter input and output power against the duty cycle.

Figure.12 shows the voltage across the converter switch and the current flow during turn off and turns on. The increase and decrease of voltage and current in both commutation modes are spike less which confirm a reduction of converter losses. The inductor current contains minimum ripple as shown in fig13.

a) b)

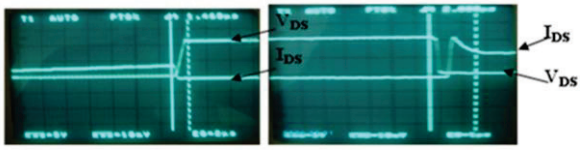

Fig12.Switch commutation I_{DS} and V_{DS}; turn off (a), turn on (b)

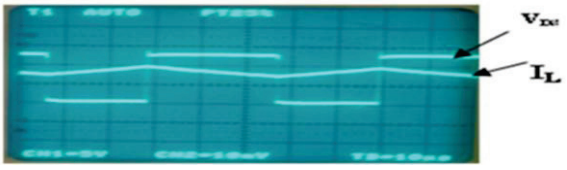

Fig.13 Inductor current I_L and V_{DS} Voltage

The tracking of power extracted from the PV generator due to duty cycle variation during operation of the system has been observed on the PC screen shown in Figures 14a, 14b, 14c; which are the instantaneous values of the

registers reserved for the variables. In the program running on EV80C196MCS Microcontroller Evaluation Board connected to the PC; the duty cycle is denoted 'ALPHA', the power is denoted 'PUISSANCE', the current is denoted 'COURANT' and the voltage is denoted 'TENSION'. The instantaneous values of the registers denoted wg_comp1, wg_comp2 and wg_comp3 are the three phase inverter PWM control.

From the three values of the duty cycle register 'alpha' and power register 'puissance' that can be read on the PC screen in (Figs14a,14b,14c), it can be concluded that the tracking process of the PVG power by the implemented MPPT algorithm is operating correctly.

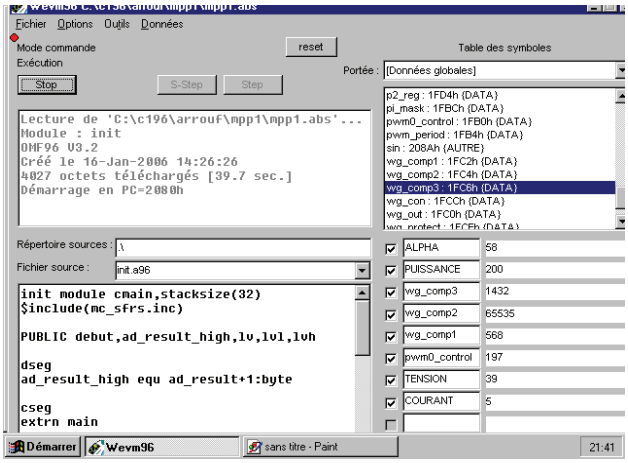

a

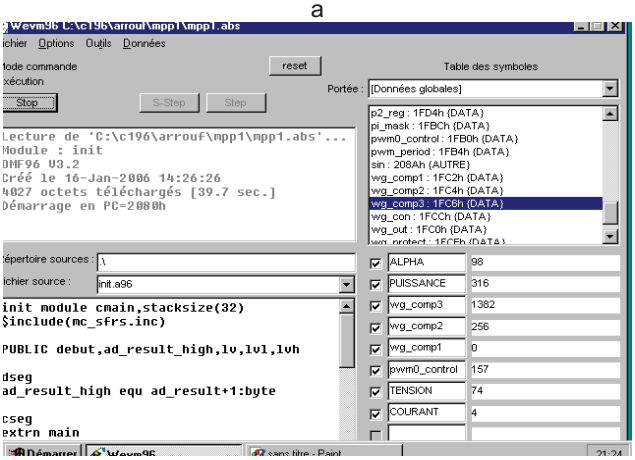

b

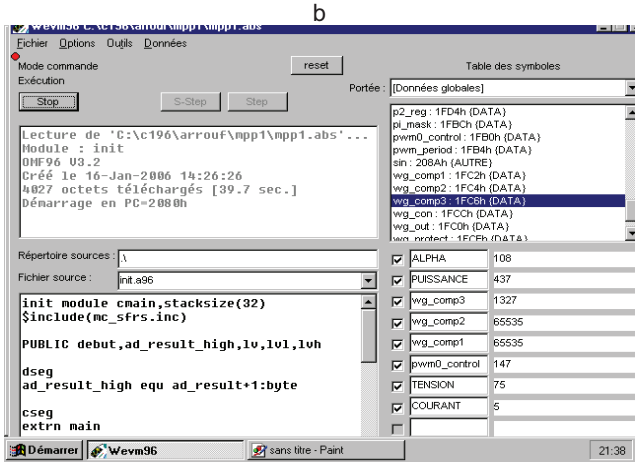

c

Fig.14 Top (a) ; middle (b) ,bottom (c) of power tracking process

Figure 15, shows the PWM waveforms of the induction motor supply voltage and current, it can be seen from the figures that the inverter PWM control is operating properly.

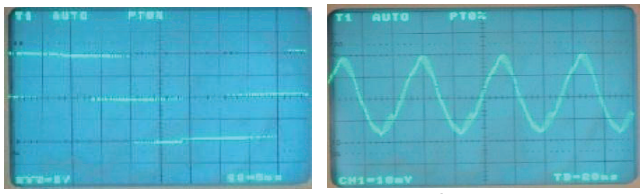

a b

Fig 15. Induction motor line to line voltage (a), line current (b)

Conclusions

A photovoltaic pumping system controlled by an EV80C196MC Microcontroller Evaluation Board has been implemented and tested. The microcontroller has the functions of the generation of PWM signals of the inverter gate driving circuits in addition to the control signal of the maximum power point tracking.

The power electronics part of the photovoltaic pumping system and their gate driving circuits were optimally designed, realized and tested.

- Step–up converter efficiency is about 94% which indicate the correct optimization of the converter, and that the tracking process of the photovoltaic generator maximum power is satisfactory.
- Inverter PWM control program is running correctly on the EV80C196MC Microcontroller and its efficiency is around 90%.

Laboratory test results of the whole system where found to agree well with the planned performance.

RREFERENCES

[1] A.B.Stambouli, "Promotion of renewable energies in Algeria : strategies and perspectives ", Renewable and Sustainable Energy Reviews 15(2011) 1169-1181.

[2] R.Duzat, "Analytic and Experimental Investigation of a Photovoltaic Pumping System", PhD thesis. Oldenburg University 2000.

[3] Yun Tiam Tan. "A Model of a PV Generation Suitable for Stability Analysis", IEEE Trans .Energy conversion 2004; 19(4): 748-755

[4] X.weindong, "A Modified Hill Climbing MPPT method for photovoltaic power systems", *35th annual IEEE Power Electronics Specialists Conference* 2004; pp1957-1964.

[5] Neil S, "Comparative study of variable seize perturbation and observation maximum power point trackers for pv systems", electric power system research 80, 2010

[6] Intel User's manual."EV80C196MC Microcontroller Evaluation Board". 1992

[7] José Fernandés –Ramous, "Improvement of photovoltaic pumping systems based on a standard frequency converters by means of programmable logic controllers", solar energy, 84, 2010

[8] D. Abdel-Karim, "Solar Powered Induction Motor-Driven Water Pump Operating on a Desert Well, simulation and field tests", Renewable Energy 2005;30: 701-714.

[9] Sun chen. "Optimal efficiency analysis of induction motor fed by variable -voltage and variable- frequency source", IEEE Energy Conversion 1992; 7(3): 537-543.

[10] M.Arrouf, "Vector Control of Induction Motor Fed by Photovoltaic Generator", Applied Energy 2003; 74 (1-2):

[11] C.Franz, "Efficiency Optimal Control for AC Drives with PWM Inverters", IEEE Transactions on Industry Applications 1985; IA-21, No.4.

Authors: *M. Arrouf, Department of Electrical Engineering, Faculy of Technology, University of Batna, Batna 05000, Algeria,E-mail: m.arrouf@hotmail.com: F. Benabid, Department of Electrical Engineering, Faculy of Technology, University of Batna, Batna 05000, Algeria,E-mail: fari_b2003@yahoo.fr .*